Organic & Biomolecular Chemistry

ROYAL SOCIETY OF CHEMISTRY

PAPER

View Article Online
View Journal | View Issue

Cite this: *Org. Biomol. Chem.*, 2025, **23**, 9950

Antiadhesive glycoconjugate metal complexes targeting pathogens *Pseudomonas aeruginosa* and *Candida albicans*†

Karolina Wojtczak, [a,b] Emilie Gillon,[c] Diana Bura,[d] Karen Richmond,[e] Megan Joyce,[e] Emma Caraher,[e] Keela Kessie,[f] Trinidad Velasco-Torrijos,[f] Cristina Trujillo, [g,d] Anne Imberty, [c] Kevin Kavanagh,[h] Gordon Cooke [e] and Joseph P. Byrne *[a,b,i,j]

Received 12th June 2025,
Accepted 20th June 2025

DOI: 10.1039/d5ob00970g

rsc.li/obc

Glycoconjugates are known to interact with carbohydrate-binding proteins involved in adhesion by pathogens, and offer opportunities to design antimicrobial agents. Metal complexes with Eu(III), Ni(II) and Zn(II) were prepared from glycoconjugate ligand **1Gal**, which binds to *P. aeruginosa*'s lectin LecA (K_d 9.6 ± 0.7 μM). *In vitro* anti-adhesive activity of these compounds was evaluated for both *P. aeruginosa* and *C. albicans*. Choice of metal ion played a crucial role in modulating anti-adhesive activity, with Eu(III) complexes most effective: [Eu·(**1Gal**)$(H_2O)_6$]$(CF_3SO_3)_3$ inhibits 60% biofilm formation by *P. aeruginosa* and [Eu·(**1Gal**)$_3$]$(CF_3SO_3)_3$ inhibits 62% of *C. albicans* adhesion to buccal epithelial cells (both at 0.1 mM). The results presented demonstrate the potential for metal coordination to significantly enhance biological activity of glycoconjugates, surpassing the effect of the ligand's modest lectin-binding affinity alone.

Introduction

The traditional approach to tackling infectious diseases has been the discovery of molecules that can kill pathogenic bacteria or fungi, by leveraging the chemical weapons evolved for the natural warfare between microbial organisms, and using them (and derivatives) in treatment of infections on living tissues be it human, animal or plant. However, many pathogens developed resistance to clinically-approved antibiotics (AMR), creating critical risks to healthcare,[1] and new antimicrobials are not being developed at an adequate rate.[2] The WHO has identified Critical Priority pathogens, for which new treatments are urgently required. These pathogens of high concern include bacteria such as *Pseudomonas aeruginosa* and the yeast *Candida albicans*.[3,4] AMR can be considered a glacial pandemic: slow moving, but vast, destructive and inexorable in its path, since multidrug-resistant strains have emerged in clinical settings, as pathogens continually evolve strategies to survive therapies. Progress in microbiology has made non-fatal strategies that instead target virulence factors, such as anti-adhesion, very attractive for development,[5–9] to prevent or reverse infection without killing the pathogen. Targeting virulence factors, rather than pathogens as a whole, is only possible with a deeper understanding of a pathogen's biology and mechanism of infection. Targeting carbohydrate-binding proteins such as adhesins and lectins may disrupt pathogen binding to cell glycans or inhibit biofilm formation. This novel anti-virulence strategy has been reported for uropathogens *Escherichia coli*,[10] for yeast *C. albicans* (CA)[11] and also for *P. aeruginosa* (PA),[6,12–16] and the fungus *Aspergillus fumigatus*,[17] which are implicated in lung infections.[5,7]

The core concept of antiadhesion strategies is that competition by soluble glycomimetics blocks pathogen adhesion to the tissue and therefore prevents the process of infection. Since the goal is to "unstick" a pathogen rather than eliminate it, as well as being non-toxic to the host, anti-adhesives should also be non-toxic to the pathogen and should not

[a]*School of Biological and Chemical Sciences, University of Galway, University Road, Galway, Ireland*
[b]*UCD School of Chemistry, University College Dublin, Belfield, Dublin 4, Ireland. E-mail: joseph.byrne@ucd.ie*
[c]*Université Grenoble Alpes, CNRS, CERMAV, Grenoble 38000, France*
[d]*School of Chemistry, Trinity Biomedical Sciences Institute, Trinity College Dublin, 152-160 Pearse St, Dublin 2, Ireland*
[e]*School of Chemical and BioPharmaceutical Sciences, TU Dublin, Ireland*
[f]*Department of Chemistry, Maynooth University, Maynooth, Co. Kildare, Ireland*
[g]*Department of Chemistry, The University of Manchester, Oxford Road, Manchester, M13 9PL, UK*
[h]*Department of Biology, Maynooth University, Maynooth, Co. Kildare, Ireland*
[i]*UCD Conway Institute for Biomedical and Biomolecular Research, Belfield, Dublin 4, Ireland*
[j]*UCD One Health Centre, University College Dublin, Belfield, Dublin 4, Ireland*

†Electronic supplementary information (ESI) available: NMR, IR, UV/Vis absorbance and emission spectra, additional ITC/SPR, DFT calculation details, and full biological assay data. See DOI: https://doi.org/10.1039/d5ob00970g

create selective pressure which would lead to the evolution of resistance; instead, mechanical expulsion is favoured through natural responses (coughing, urination *etc.*). Another advantage of this strategy is that it is effective against already resistant strains. Mathematical models predict anti-adhesion combined with antibiotic treatment is effective at removing resistant bacterial infections in synergy with each other;[18] this has been shown *in vitro* with dendrimers targeting bacterial lectin LecB.[19] Practical trials exist in hospital settings where combined administration of carbohydrate inhalations and antibiotics to people with Cystic Fibrosis accelerated the clearance of chronic PA infections in the airways when compared to antibiotic-only treatment.[20,21] Often, the antiadhesive glycoconjugates can also prevent the formation of bacterial biofilms which are key to pathogenic behaviour and are known to decrease the susceptibility of bacteria to treatments.[22]

Progress has been made in the last two decades to develop glycoconjugates as high-affinity inhibitors for bacterium PA's two soluble lectins LecA and LecB,[8] which are selective for galactosides and fucosides/mannosides, respectively. Nanomolar affinities are achieved by multivalent presentation of carbohydrates on scaffolds as diverse as peptide dendrimers, calixarenes and nanoparticles,[13,14,19] as well as simpler carefully-designed lower valency druglike molecules.[16,23,24] Affinity is not directly predictive for antiadhesive activity, but a range of successful antiadhesive compounds were recently reviewed by Titz and co-workers,[6] while Vidal and co-workers reported glycoconjugate treatment providing protection against PA lung infection in an *in vivo* mouse model.[14]

While only 27 treatments are in the clinical pipeline for WHO priority bacterial pathogens,[2] in the case of antimycotic agents the situation is also limited:[4] three new antifungals are currently in the pipeline, two of them first-in-class.[25] Much innovation in the field is centred on novel formulations of Amphotericin-B such as its incorporation into nanoparticles[26] or on monoclonal antibody therapies.[25–27] Fungi represent a smaller proportion of infections however they continue to accumulate resistance to current treatments; an anti-adhesive strategy presents an attractive opportunity for development as anti-mycotics if suitable targets are identified. Velasco-Torrijos and co-workers reported a library of molecules, including **3** and **4** (Fig. 1), showing that suitably presented divalent galactosides have anti-adhesive effects against CA.[11,28,29] Bis-triazole **3** was the first glycoconjugate known to inhibit CA's adhesion to human Buccal Epithelial Cells (BECs) (45% *vs.* controls). Structure–activity relationships indicate a mechanism that is driven by the identity of the carbohydrate motif, and while the precise molecular target is not yet identified, it is likely a cell wall adhesin.[11] A follow-up study varied the central scaffold to lock a "closed" conformation of the sugars, and norbornene-based derivative **4** had comparable activity albeit requiring much higher concentrations.[28] A multivalent peptide-based dendrimer presenting four copies of motif **3** was constructed, leveraging the glycoside cluster effect, and resulted in an increase in activity at a much lower concentration than its predecessors.[29]

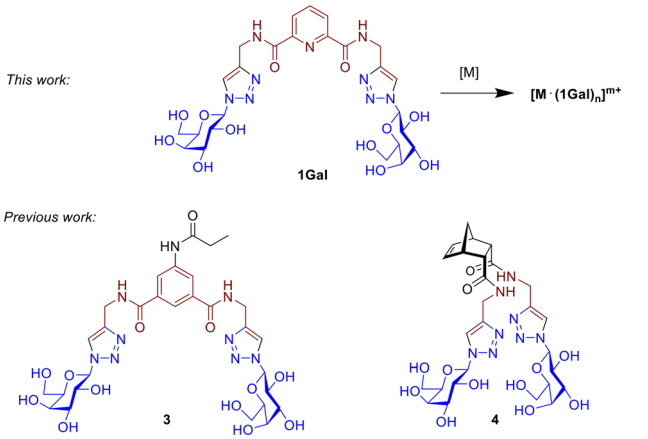

Fig. 1 Structure of ligand **1Gal** and its metal complexes, compared with other previously-reported digalactoside compounds **3** and **4**.

Metallodrugs such as Salvarsan and Pepto-Bismol were among the very first antimicrobial agents used to consciously treat infections in modern medicine.[30] After the discovery of penicillin and the advent of small-molecule antibiotics, metallodrugs were relegated to a secondary league, and only viewed as viable candidates for development after the success of Cisplatin in the treatment of cancer since the 1970s.[31] Metallodrugs continue to be an underexplored and underdeveloped class of molecules with immense potential; a recent assessment of the proportion of inorganic complexes submitted to the CO-ADD initiative showed 27% of complexes had antimicrobial activity, while only 2% of the purely organic molecules submitted demonstrated any antimicrobial effects.[32,33] However, no metallodrugs are currently in clinical trials as antimicrobials, despite approval of silver sulfadiazine and bismuth tribromophenate.[30,32,34,35] Schiff base transition metal complexes are reported to kill CA, with a Ni(II) complex particularly effective.[36] Ruthenium complexes are best represented in the antibacterial metallodrug research, generally being more active against Gram-positive bacteria (*e.g.* MRSA)[37–39] than Gram-negative species like PA.[37,40–42] Machine learning is also being used to predict antimicrobial metal complexes, as a potential method of metallodrug discovery.[43]

Glycoconjugate metallodrugs have been considered as targeted anti-cancer agents,[44] however targeted antiadhesive strategies with metal complexes based on glycoconjugates has not be widely explored. Au(I)-based drug Auranofin has shown activity against *S. aureus*,[45] and glucose-containing Ir(III) complexes have been reported to inhibit PA biofilm at 16 μg mL^{-1} with a MIC of 4 μg mL^{-1},[46] however it is unclear in either case if the mechanism of action of these involves carbohydrate recognition by lectins/adhesins. Previous work published by the Byrne Group reported the first example of a metal ion used to template glycoconjugate ligands, which inhibited biofilm formation by targeting the galactophilic lectin LecA expressed by PA;[47] it was found that templating the glycoconjugate

ligands into a multivalent topology was required for activity not seen for ligands alone, while the Ru(II) played only a structural role. The work presented here investigates activity of related glycoconjugate derivatives **1** (Fig. 1), based on the **dpa** (dipicolinic acid) motif, a class of ligand widely used to coordinate metals with diverse properties and geometries including lanthanide and transition metals.[48,49] The combination of glycoconjugate ligands with targeting epitopes curated to interfere with lectins or adhesins, and the presentation topologies metal complexes presents a family of new potential antiadhesive agents.

Results and discussion

Affinity of 1Gal for LecA

The synthesis of digalactoside **1Gal** was previously described in a study of luminescent lectin-sensing by Tb(III)-glycoconjugate complexes.[50] The complex of **1Gal** was not an effective sensor for LecA, but analogues with flexible spacers between the carbohydrate motif and the triazole function as 'switch-on' sensors for unlabelled bacterial lectin LecA.[50] We have since further investigated affinity of **1Gal** by isothermal calorimetry (ITC) and surface plasmon resonance (SPR) to establish that this compound has surprisingly high affinity for PA's galactophilic lectin, considering the short spacing between galactose epitopes, precluding chelate binding.[24] In ITC experiments (Fig. 2), binding data for **1Gal** indicated this digalactoside binds to LecA in a 1 : 1 stoichiometry, only availing of one galactose epitope at a time, which is unsurprising, due to the relatively wide spacing of neighbouring receptor sites in the LecA tetramer (*ca.* 29 Å).[51] An average K_d of 9.6 ± 0.7 μM for LecA was determined. The interaction had a typical enthalpy for a single carbohydrate recognition event with LecA of about −30 kJ mol^{-1}. Moreover, SPR data, determined by immobilising LecA on a chip to investigate kinetic interactions also gave a low micromolar affinity of 6.6 ± 0.5 μM, using a steady-state fitting model and 5.9 ± 0.1 μM by kinetics fitting model. A more flexible related ligand **5** (Fig. S21, ESI†), with a triethyleneglycol linker[50] had marginally better affinity by ITC (6.5 ± 0.1 μM) and comparable K_d by SPR (6.0 ± 1 μM) indicating that for this motif, the added length and flexibility conferred by the linker does not affect affinity to the lectin to a major extent, while lanthanide-coordination by either ligand has minimal impact on K_d.[52]

These experiments establish that **1Gal** has lectin-targeting motifs that bind to LecA (and likely other galactose-binding proteins), thus opening possibilities to test this ligand as part of inorganic complexes for bacteriostatic or antimicrobial effects. Its low micromolar affinities, achieved through single-site binding, are modest compared to several carefully designed mono- and di-valent examples, of varying degrees of synthetic complexity, but review of the field has established that affinity is not directly predictive of antiadhesive or other biological effects.[8,15,23] Moreover, this high-yielding and straightforward preparation allows efficient modular ligand synthesis without sacrificing much affinity, encouraging us to develop derivatives with other carbohydrate moieties by lever-

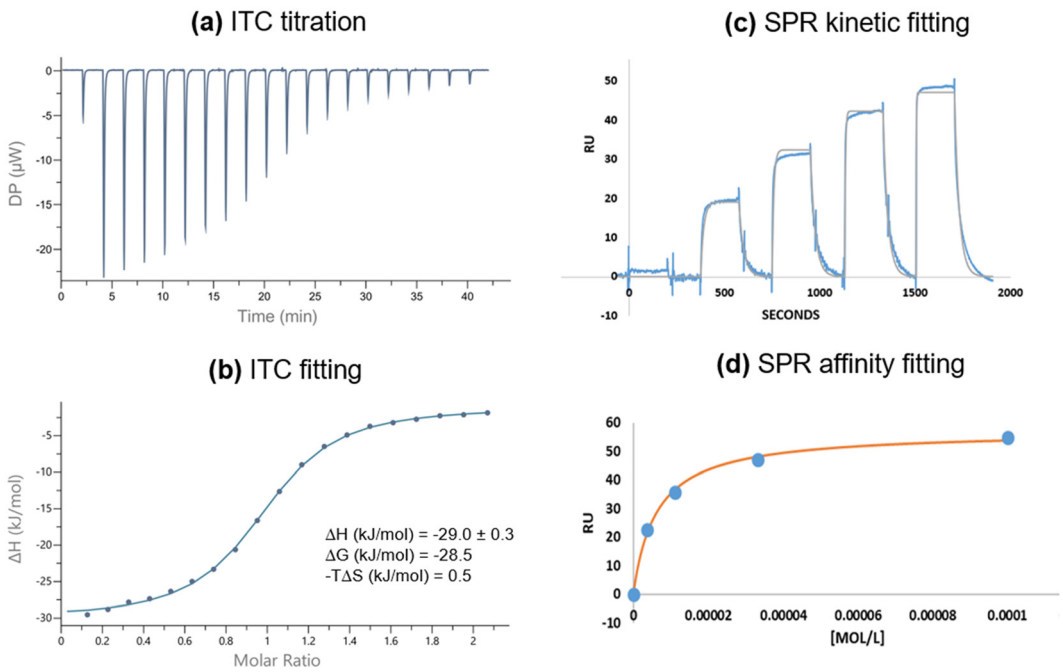

Fig. 2 Biophysical analysis of interactions between **1Gal** and LecA. (a and b) Isothermal calorimetry titration and fitting in 10 mM Tris/HCl buffer (pH 7.2, 100 mM NaCl, 10 μM $CaCl_2$), [LecA] = 300 μM; (c and d) surface plasmon resonance kinetic and affinity fitting, carried out in PBS buffer (10 mM phosphate buffer pH 7.4, 2.7 mM KCl, 137 mM NaCl, 100 μM $CaCl_2$, 0.05% Tween 20) with [**1Gal**] = 0–100 μM.

aging the efficiency of click reactions, and complex these to a variety of metals as potential anti-biofilm agents targeting PA's lectins.

Synthesis of glycoconjugate ligands

The dipicolinic amide motif (**dpa**) is well known tridentate coordinating motif for lanthanides and transition metals.[48,49] Ligand **1Gal** was prepared as described previously,[50] while for this study glucose and lactose analogues (**1Glc**, **1Lac**) were also synthesised (Scheme 1). In brief, fully acetylated saccharide azide derivatives were prepared conveniently from acetylated α-bromoacetylglycopyranosides and NaN_3. From these azides, protected triazoles $\mathbf{1}^{\mathbf{OAc}}$ were prepared through Cu(I)-catalysed azide–alkyne 'click' reactions (CuAAC) with alkyne **2**. Acetylated triazoles were quite polar and could be easily purified by flash chromatography in ethyl acetate, with good yields (60–70%).

The triazoles were then deprotected under Zemplén conditions to obtain pure ligands **1** as white solids in high yields (>95%) at a scale of hundreds of milligrams; facile isolation makes them convenient synthetic targets. Disappearance of a characteristic ester C═O band in IR spectrum of **1Gal** compared to $\mathbf{1Gal}^{\mathbf{OAc}}$ confirmed deprotection (see ESI†), alongside absence of acetyl CH_3 resonances in ^{1}H NMR. Each glycoconjugate ligand's ^{1}H NMR spectrum shows a single set of peaks, corresponding to formation of single anomers without epimerisation, evidenced by coupling constants of the anomeric proton resonances at of 9.2 Hz for **1Gal** and **1Glc**, and 9.2 Hz (lactoside glucose) and 7.8 Hz (lactoside terminal galactose) for **1Lac** respectively. The lactoside is linked to the triazole *via* the glucoside anomeric position thus making it more deshielded than the galactoside moiety. High resolution mass spectrometry (ESI+, Q-TOF) was used to further characterise the ligands and in all cases the mass found agreed with the calculated *m*/*z* of the ion. For instance, for **1Glc**, calculated for $C_{25}H_{33}N_9O_{12}^+$ $[M + H]^+$ *m*/*z* = 652.2326; found *m*/*z* = 652.2320.

Preparation of metal complexes of 1

Complexes with transition metals were assembled by reflux in MeOH solution of **1Gal** with $NiCl_2$ or $Zn(OAc)_2$, in a 2 : 1 molar ratio. Complexes formed readily and could be isolated by simple evaporation of the solvent or centrifugation followed by drying, with no evidence of unreacted ligand. All complexes had distinct ^{1}H NMR spectra featuring characteristic broadening of peaks, particularly those corresponding to the **dpa** motif and anomeric protons. IR spectra showed slight shifts in characteristic peaks corresponding to the amide C═O stretch, and the fingerprint region to varying degrees (Fig. S20, ESI†). UV-Vis spectra for both complexes, Fig. 3, show a structured absorbance feature with λ_{max} = 274 nm, with stronger absorbance than the ligand at the same concentration, and a band at λ_{max} = 224 nm, features which are typical for **dpa** derivatives.

To establish the self-assembly behaviour of **1Gal** with lanthanide Eu(III) and its ability to form complexes, a self-assembly titration was performed by adding aliquots of Eu $(CF_3SO_3)_3$ to a 2×10^{-5} M aqueous solution of **1Gal** and monitoring changes in the UV-Vis absorbance and Eu(III)-centred emission spectra (Fig. S24, ESI†). Changes in absorbance spectra were modest, with hyperchromic shift in the spectrum around the maximum at 223 nm and higher energies, and only slight increase in absorbance in the peak with λ_{max} = 274 nm. Upon addition of Eu(III), the non-phosphorescent ligand sensitised metal-centred emission with characteristic line-like bands at 591, 614, 625 and 695 nm which correspond to $^5D_0 \rightarrow {}^7F_{1-4}$ transitions, which increased in intensity with lanthanide ion concentration. Global stability constants were estimated by fitting spectroscopic data by non-linear regression (ReactLab Equilibria, Jplus Consulting Pty Ltd) to a model including the formation of Eu: $\mathbf{1Gal}_n$ (*n* = 1,3) self-assemblies in solution. When 1 : 2 assembly was included in the model, the fit did not converge. The ground state data indicated $\log\beta_{1:1}$ = 6.4 and $\log\beta_{1:3}$ = 16.1 ± 0.2, while fitting data from the emission of the excited state broadly agreed, with $\log\beta_{1:1}$ = 5.5 and $\log\beta_{1:3}$ = 14.9 ± 0.2. These stability constants with Eu(III) agree closely with those obtained with Tb(III) for related ligand structures by us and others.[50,53,54]

Based on these self-assembly studies, complexes with Eu(III) were prepared with 1 : 1 and 1 : 3 stoichiometries by reflux of $Eu(CF_3SO_3)_3$ and **1Gal** in the appropriate ratios, followed by evaporation to give white solids which luminesce red-orange under UV irradiation (Fig. S26, ESI†), namely $[Eu{\cdot}(\mathbf{1Gal})(H_2O)_6]$

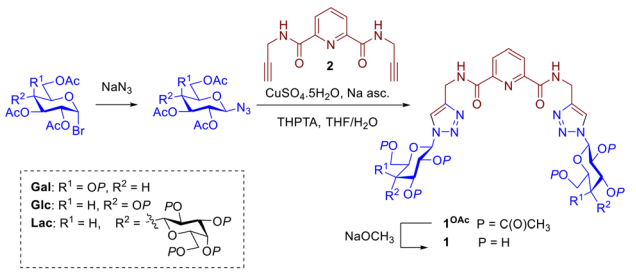

Scheme 1 Synthesis of **dpa** glycoconjugate ligands **1Gal**, **1Glc** and **1Lac**.

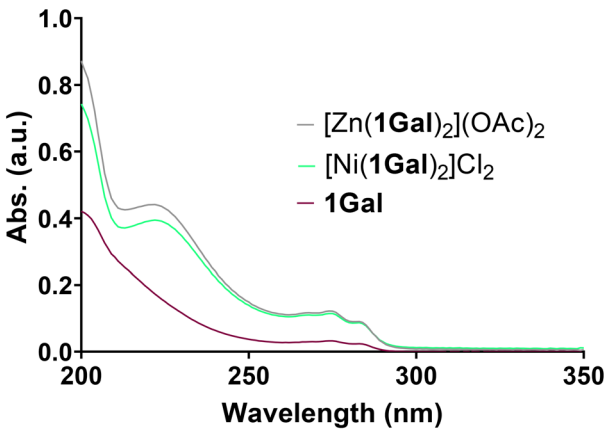

Fig. 3 UV-Vis absorbance spectra of transition metal complexes of **1Gal**.

$(CF_3SO_3)_3$ and $[Eu{\cdot}(\mathbf{1Gal})_3](CF_3SO_3)_3$, each demonstrating luminescent signals whose decay curves fit to a single exponential curve.[55] Attempts to prepare 1 : 2 complexes failed, giving instead a mixture of the 1 : 1 and 1 : 3 complexes. Analogous complexes with **1Glc** and **1Lac** were also prepared. Due to the paramagnetic nature of the lanthanide ion, ^{1}H NMR spectra (500 MHz, D_2O) of these complexes were broadened and shifted compared to those of the corresponding ligands (Fig. S11 and S12, ESI†). Emission spectra of the isolated complexes demonstrate characteristic Eu(III)-centred emission as seen for the self-assembly studies. Quantum yields (Φ) of these complexes were determined by a relative method, using $Cs_3[Eu{\cdot}(\mathbf{dpa})_3]$ as a secondary standard,[56] and it was found that the 1 : 1 complexes were more emissive than trileptic complexes with Φ = 4% for the 1 : 1 complex of **1Gal**, approximately double that for the 1 : 3 complex (Table 1).

Biological activity against *Pseudomonas aeruginosa*

Based on the affinity of ligand **1Gal** for LecA, it was anticipated that this series of glycoconjugate complexes with varying topologies and stoichiometries might interact with PA with antimicrobial or anti-virulence effects. Initially, bactericidal behaviour was assessed by testing the ability of galactosides incubated with bacteria at a range of concentrations from 1 μM to 10 mM to inhibit growth of PAO1 strain of the bacterium, as compared with bacteria-only control and a positive control (where 1 μg mL^{-1} of commercial antibiotic ciprofloxacin was added). No biologically-significant toxicity was seen for **1Gal**, or any of its complexes, even at concentrations as high as 10 mM, see Fig. 4a. The zinc and nickel complexes of **1Gal** were both found to be completely innocuous to the bacteria, even at high concentrations (Fig. S27, ESI†). Interestingly, while each metal salt precursor ($Eu(CF_3SO_3)_3$, $NiCl_2$ and $Zn(OAc)_2$) showed toxicity at 10 mM, this was not replicated by their complexes or by salts at lower concentrations for Eu(III) and Zn(II), illustrating that coordination chemistry modulates the biological effects of the metal ion, and complexes are sufficiently stable to dissociation to demonstrate their own biological activity profile.

Since these complexes have negligible toxicity, potential anti-virulence activity was also probed by *in vitro* assay. Biofilm inhibition was investigated for all galactoside compounds by crystal violet assay,[57] and percentage inhibition of biofilm measured as optical density (OD) at 590 nm, normalised to the mean of a bacteria only control (all concentrations shown Fig. S28, ESI†). Ligand **1Gal** did not show any biofilm inhibition, even at higher concentrations, nor did the Ni(II) complex, while alternative ligands with glucosyl or lactosyl epitopes were also ineffective at biofilm inhibition. Non-toxic complex $[Zn{\cdot}(\mathbf{1Gal})_2](OAc)_2$ only showed significant inhibition at 1 mM (45%, $p < 0.01$) and not at 10 mM, this counterintuitive and non-linear drop in inhibitory effect may be explained by zinc being an endogenous metal for organisms, which upon higher concentration could be abstracted from the complex by the bacteria and used as a micronutrient.[58]

The biofilm inhibition activity of monoleptic complex $[Eu{\cdot}(\mathbf{1Gal})(H_2O)_6](CF_3SO_3)_3$ was of most note, as it persisted with significance to lower concentrations: it showed a remarkable 60% biofilm inhibition at 0.1 mM, and 48% even as dilute as 0.01 mM ($p < 0.0001$), Fig. 4b. Control compounds of the same complex structure with **1Glc** or **1Lac** did not demonstrate decrease in biofilm formation (Fig. S28, ESI†), suggesting that this activity is facilitated by the micromolar interactions of this galactoside with LecA established by ITC above, since LecA is known to play a role in biofilm formation.[6,59] While the complexes with 1 : 1 stoichiometry demonstrate strong effects, the Eu(III) complex with 1 : 3 stoichiometry also had more modest effects with 39% biofilm inhibition when bacteria were incubated with 0.1 mM of the complex, despite presenting additional galactoside epitopes. This suggests that Eu(III) plays an important role in the mechanism of inhibition but it is unlikely that the biofilm inhibition

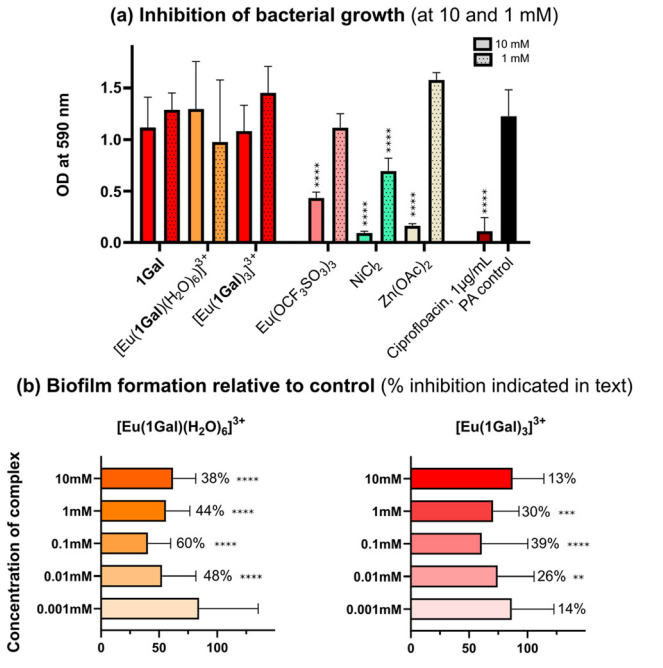

Fig. 4 (a) Bactericidal activity to PA for ligand **1Gal**, its Eu(III) complexes and the precursor metal salts (at 10 mM and 1 mM) compared to positive and negative control; (b) effect of Eu(III) complexes on biofilm formation (±SD, compared to control experiments with PA alone), with percentage inhibition indicated in text and statistical significance indicated by asterisks (One-way ANOVA). Biofilm formation measured by crystal violet assay (N = 5, 3 replicates per experiment).

Table 1 Quantum yields of Eu(III) complexes of **1**

Complex	Φ (%)
$[Eu{\cdot}(\mathbf{1Gal})(H_2O)_6](CF_3SO_3)_3$	3.8
$[Eu{\cdot}(\mathbf{1Glc})(H_2O)_6](CF_3SO_3)_3$	6.2
$[Eu{\cdot}(\mathbf{1Lac})(H_2O)_6](CF_3SO_3)_3$	4.4
$[Eu{\cdot}(\mathbf{1Gal})_3](CF_3SO_3)_3$	1.8
$[Eu{\cdot}(\mathbf{1Glc})_3](CF_3SO_3)_3$	3.2
$[Eu{\cdot}(\mathbf{1Lac})_3](CF_3SO_3)_3$	0.4

is caused simply by chelation between carbohydrate-binding active sites by the ligands, as the 1 : 3 complex does not benefit from the 'glycocluster effect'. It is worth highlighting that even though the affinity of the ligand for LecA is moderate compared to some other known examples, not all potent LecA ligands disrupt biofilm behaviour, and this complex's biofilm inhibition effect emerged upon complexation to a particular metal ion, and so is not reliant solely on the potency of lectin inhibition.

These results point to an interaction with PAO1 bacteria *in vitro* for this range of complexes that demonstrate low toxicity, but nonetheless in the case of Eu(III) complexes in particular, metal coordination gives rise to a carbohydrate-targeted biofilm inhibition effect that is noteworthy, particularly in the case of complexes with a 1 : 1 stoichiometry. The largest effect measured at subinhibitory concentration, at approximately 50% decrease in biofilm formation *vs.* control compares favourably with Ru(II) and Ag(I) complexes reported previously.[41,47,60]

Given that antiadhesive activity here relies on the identity of the carbohydrate epitope as well as the metal ion, it is likely that some of these complexes might also be effective for antiadhesive therapeutic effects against other pathogens with relevant receptors for galactosides.

Molecular modelling of ligand 1Gal and its complexes

Carbohydrate-presentation plays an important role in glycoconjugate–protein interactions, so to gain insight into the structure of these compounds, and how complexation might influence galactoside presentation, DFT calculations were carried out to predict the lowest energy conformations in water (SMD method). Noting structural similarity of ligand **1Gal** to previously published compounds possessing a bis-galactoside motif, such as **3** (Fig. 1), we hypothesised that **1Gal** and its complexes, in addition to the PA biofilm inhibition already described, also have potential for antiadhesive activity against fungus CA.[11,28,29] The most stable conformation of **1Gal** was found to be a closed 'basket' configuration (Fig. 5), which is analogous to that of the previously-reported molecules **3** and **4** with known CA antivirulence activity.[28] Calculated energies of the conformers and the inter-anomeric carbon distances in each correspond closely, being 5.90 Å for the most stable conformer (Fig. S30, ESI†). This suggested that the **dpa** derivative and its metal complexes have potential for anti-adhesive activity against CA. Complexation to metals gives access to topological presentation patterns inaccessible or difficult to access with purely organic molecules.[13,19,29] The most stable conformer of the Eu(III) complex shows similar overall configuration and inter-anomeric carbon distances (6.14 Å) to the ligand, whereas in calculated Ni(II) and Zn(II) complex conformers, this distance (within the same ligand) is extended by *ca.* 1 Å. This variation, along with the change in multivalency may interplay with the varying biological activity observed for these systems.

Adhesins belonging to yeasts of the Candida genus are known and lectin-like interactions are recognised as one of the three types of adhesive interactions along with integrin mediated protein–protein interactions and as of yet undefined interactions.[61,62] Lectin-like interactions CA's surface are often attributed to mannoprotein and fucoside recognition, with some examples also citing GlcNAc as epithelial cell receptors,[63,64] but to date the exact protein responsible for galactoside recognition in CA is not known, therefore the characterisation of interactions at a molecular level (*e.g.* ITC) is not yet possible. Nevertheless, several studies, including the data presented below, demonstrate adhesion to human buccal epithelial cells (BECs) can be significantly inhibited by glycoconjugates with galactose epitopes (particularly divalent galactosides), providing potential medicinal value at early stages of infection.

Biological activity against *Candida albicans*

To probe the interactions of **1Gal** with CA, two types of assays were carried out: a pre-treatment assay, and a competition assay. These experiments allowed insight into the effects of digalactosides on protecting human BECs from adhesion and for competing with adherent fungi, respectively. These data are directly comparable to existing examples in the literature.[11,28,29]

The pre-treatment exclusion assay, Fig. 6a and b, 0.1 mM **1Gal**, was incubated with CA before exposing BECs to the

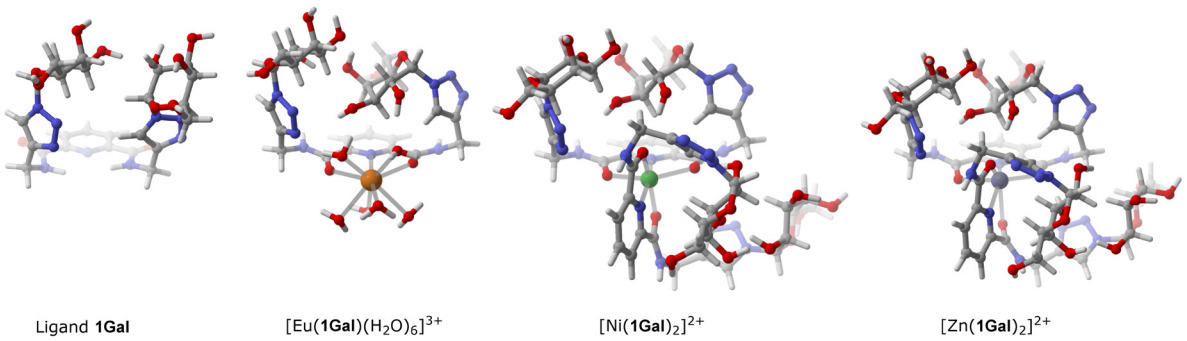

Fig. 5 Most stable conformer structures calculated by DFT for **1Gal** and its complexes. Details of parameters given in the experimental section; additional illustrations in ESI.†

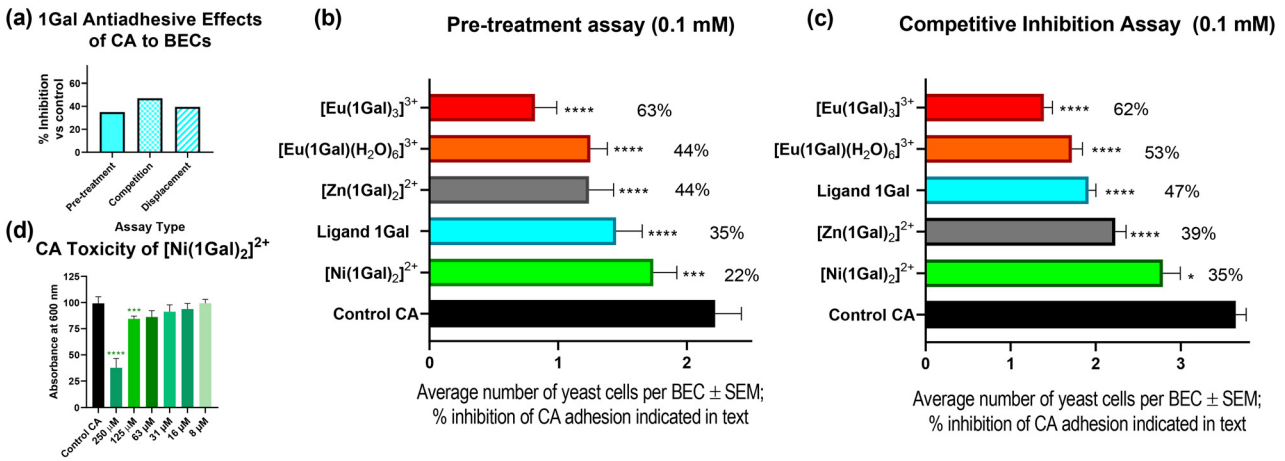

Fig. 6 Biological assays of **1Gal** and its complexes against *C. albicans* (CA). (a) Inhibition of adhesion of CA to BECs by **1Gal** measured by three different assay types; (b) inhibition of CA in a pre-treatment exclusion assay; (c) inhibition of adhesion of CA in a competition assay, compared to control experiments. (d) Toxicity of Ni(II) complex towards CA at low concentrations.

yeast; this assay showed decrease in CA cells attached to the human cells: 35% less than the control. While in a competitive assay, where BECs were co-incubated with yeast cells and the glycoconjugate, **1Gal** achieved a 47% decrease in adhesion *versus* control ($p < 0.0001$), Fig. 6c. This ligand compared very well with previously reported activity of **3**.[11] Compound **3** gave *ca.* 35% reduction in both assays, while displacement assays with both **1Gal** and **3** also showed comparable results (ESI†).

Having confirmed the effectiveness of the **dpa**-based ligand scaffold, we examined the impact complexation with a variety of metals had on CA yeast cells and their antiadhesive activity. Since toxicity is a concern in medicinal chemistry when proposing metallodrug candidates,[30] particularly as antiadhesives, toxicity assays were first performed to identify any fungicidal potential for this series of complexes (Fig. S33, ESI†). Upon incubating CA culture with various concentrations of **1Gal** and its complexes, the nickel(II) complex was the only one to inhibit growth with any statistical significance, doing so even at concentrations as low as 63 μM (Fig. 6d). One-way ANOVA analysis was performed at each concentration to determine statistical significance of results ($p < 0.1$). Europium(III) complex $[Eu{\cdot}(\mathbf{1Gal})_3](CF_3SO_3)_3$ exhibited no toxicity, a very encouraging result given its effectiveness against PA above, and likely impact on CA adhesion.

In the pre-treatment exclusion assay, Fig. 6b, where each complex was tested at 0.1 mM, the Ni(II) complex was less effective than the ligand alone (22% inhibition), and it was observed that the yeast cells were particularly small compared to other experiments, a result that may be explained by this complex's toxicity, Fig. 7a and b. Indeed, under the same assay conditions, $NiCl_2$ alone also gave rise to 18% inhibition (ESI†), suggesting that biological activity here is likely metal-driven.

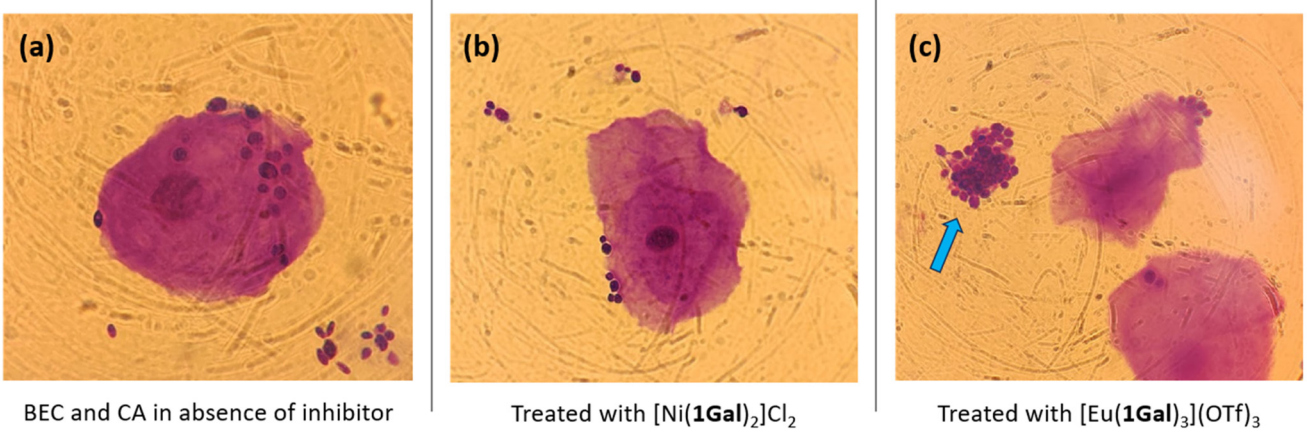

Fig. 7 Optical microscope images (100×) of human buccal epithelial cells (BECs) in the presence of *C. albicans* (a) without any inhibitor (control sample); (b) in competition assay with the Ni(II) complex, demonstrating smaller fungal cells; (c) in competition assay with 1 : 3 Eu(III) complex, demonstrating of clumping of *C. albicans* cells (indicated with arrow) and human BECs with minimal fungal adhesion.

On the other hand, non-toxic complexes $[Eu\cdot(\mathbf{1Gal})(H_2O)_6](CF_3SO_3)_3$ and $[Zn\cdot(\mathbf{1Gal})_2]Cl_2$ both outperformed the ligand (44%), without any unusual morphology of the fungal cells. The most effective antiadhesive was trileptic complex $[Eu\cdot(\mathbf{1Gal})_3](CF_3SO_3)_3$, which inhibited 63% of adherence of CA cells to the BECs. This result at 0.1 mM was comparable with a tetravalent peptide-based dendrimer derivative of **3** which inhibits 64% of adhesion at 0.212 mM, but with much simplified synthetic procedure in the case of this work, merely requiring the assembly of lower-valency ligands in the presence of a metal ion, and slightly lower concentration.[29] Importantly, control experiments with the metal salt precursors showed negligible antiadhesive properties with $Eu(CF_3SO_3)_3$ alone (ESI†), indicating that increased activity arises from enhancing the capacity of the glycoconjugate to interact with CA.

Competition assays with the same metal complexes, Fig. 6c, demonstrated very similar trends to those seen above. As in the pre-treatment assay, the Eu(III) complexes, when added to BECs at the same time as the yeast compete most effectively to prevent adherence of CA. The 1 : 3 complex inhibits 62% of adhesion and the 1 : 1 complex 53%. The Zn(II) complex also had an inhibitory effect of *ca.* 40%. In the presence of the 1 : 3 Eu(III) complex, clumping of fungal cells was observed under microscope, Fig. 7c. This had also been observed in the pre-treatment assay. It may point towards a multivalent-glycocluster mechanism of action for this compound relying on presentation of multivalent digalactoside epitopes in three-dimensions, bringing together several pathogen cells, thereby preventing their adhesion to the human cells. This clumping, not observed for the slightly less antiadhesive 1 : 1 complexes, might present challenges *in vivo*, and thus must be considered carefully in further exploration of these systems. We are currently developing analogues of these ligands to include more conjugated chromophores which might allow for excitation of probes with blue light for potential fungal imaging applications; this may give further insight into the precise protein target of this class of anti-adhesive.

Conclusions

We have demonstrated that metal coordination chemistry is able to assemble glycoconjugate ligands in such a way as to enhance antiadhesive effects from binding to pathogens' carbohydrate-binding proteins, in the case of *P. aeruginosa* and *C. albicans* (both WHO Critical Priority pathogens). Galactoside **1Gal** has moderate micromolar binding affinity for PA's lectin LecA, but while the ligand alone doesn't demonstrate biofilm inhibition for this bacterium *in vitro*, the Eu(III) complexes do so at subinhibitory concentrations (up to 60% for the 1 : 1 complex). DFT modelling of these compounds suggested that the ligand and complexes shared structural properties with previously-reported anti-CA agents, and indeed **1Gal** and its complexes with Ni(II), Zn(II) and Eu(III) also display antiadhesive effects on the fungus' interactions with human BECs *in vitro*, with the most effective agent again being the 1 : 3 Eu(III) complex. This lead complex inhibits or outcompetes >60% of yeast adhesion, and demonstrates clumping of the yeast cells. These results indicate that while carbohydrate epitopes target pathogens' carbohydrate-binding proteins, this alone may not directly translate into antiadhesive effects – this is pathogen specific, and antiadhesive activity may be unlocked or modulated through choice of coordinated metal ions. Eu(III) complexes, in particular, show promise from this study and we are seeking to optimise these structures' photophysical profile and lectin-affinity to allow for future use of these luminescent compounds for imaging in more detailed models of lectin-mediated pathogenesis (*e.g.* biofilm flow cell confocal microscopy, study of epithelial cell adhesion/toxicity), and to probe whether this activity is shared across the range of lanthanide(III) complexes, or if Eu(III) plays a unique role in the mode of action of these complexes. Moreover, optimised complexes may sensitise these and other pathogens to adjunct therapy approaches with traditional antibiotics. These promising results for glycoconjugate coordination compounds open up opportunities to develop further antiadhesive metal complexes, with variation in topology, ligand design and metal-centred activity, such as redox activity.

Experimental

General experimental details

NMR spectra were obtained on a Varian VNMRS 500 MHz 54 mm AR Spectrometer (UoG) operating under VnmrJ software, JEOL 400 MHz NMR ECX-400 Spectrometer (UoG), and Varian VnmrS 400 MHz spectrometer (UCD). Chemical shifts (δ in ppm, J in Hz) were referenced to residual solvent resonances and are reported downfield from $SiMe_4$. Deuterated solvents $CDCl_3$, D_2O, DMSO-d_6 were obtained commercially and used without further purification. Spectra were visualised and analysed using MestReNova software. Infrared spectra were obtained on a PerkinElmer Spectrum 400 FTIR/FT-FIR spectrometer equipped with a universal ATR accessory. High resolution mass spectroscopy was performed on an Agilent 6530 Accurate Mass Q-TOF LC/MS coupled to an Agilent 1290 Infinity UPLC system (UoG), Agilent 6546 Quadrupole Time-Of-Flight MS System coupled with an Agilent 1260 Infinity Prime II LC system (UCD) and on a Bruker 'autoflex maX' MALDI TOF/TOF system equipped with a HTX Technologies TM-Sprayer (using Super-DHB matrix). TLC experiments were performed using aluminium sheets pre-coated with silica gel 60 (HF254, E. Merck, Darmstadt, Germany). Chromatography was performed with silica gel 60 mesh (Sigma Aldrich, Wicklow, Ireland). Reactions performed under microwave irradiation were carried out in a CEM Discover-SP Microwave Reactor, 2012 model, in the appropriate bespoke vessels (UoG). All starting materials were obtained from commercial sources and used without further purification, unless otherwise stated. Dialkyne **2**,[65] glycopyranose azides,[66] and dpa-based compounds ($\mathbf{1Gal^{OAc}}$, **1Gal** and **5**)[50] were prepared as previously reported.

Expression and purification of recombinant LecA were performed as previously described[67] and the protein was lyophylized. ITC experiments were performed on an MicroCal ITC200 instrument by Malvern Panalytical and all data analysis was performed using MicroCal PEAQ-ITC analysis software (Malvern Instruments). SPR measurements were performed on a Biacore™ X100 instrument using Biacore CM5 gold chips and data analysed with the analysis software (Biacore). All stock solutions were made from lyophilised material prior to use.

Synthetic procedures

General procedure for the synthesis of ligand precursors $\mathbf{1}^{\mathbf{OAc}}$ *via* CuAAC click chemistry. Scaffold **2** (1 equiv.) and the corresponding sugar azide (2 equiv.) were dissolved in 5 mL of THF. To this solution was added 2.5 mL of an aqueous solution containing $CuSO_4{\cdot}5H_2O$ (0.015 g, 0.06 mmol), sodium ascorbate (0.024 g, 0.12 mmol) and THPTA (0.049 g, 0.12 mmol). The resulting reaction mixture was irradiated in a microwave reactor at 80 °C for 45 min and then stirred overnight at rt. Reaction mixture was diluted with EtOAc and 1 M EDTA/NH_4OH was added. The aqueous phase was extracted twice more with EtOAc, organic layers combine and dried over $MgSO_4$. Specific purification and characterisation for each ligand are given below.

$\mathbf{1Glc}^{\mathbf{OAc}}$. Synthesised following the general procedure from scaffold **2** (0.106 g 0.44 mmol) and β-acetylazidoglucose (0.330 g, 0.88 mmol). Solvent removed *in vacuo* and crude recrystallised from THF : H_2O (2 : 1) and filtered to obtain white crystals. Yield 0.516 g, 0.52 mmol (59%). HRMS (QTOF ESI+) calcd for $[M + H]^+$ $C_{41}H_{49}N_9O_{20}^+$ m/z = 988.3167, found m/z = 988.3171 and $[M + Na]^+$ $C_{41}H_{49}N_9O_{20}Na^+$ m/z = 1010.2986, found m/z = 1010.2993; ^{1}H NMR (500 MHz, DMSO-d_6): δ = 9.94 (t, J = 6.3 Hz, 2H, NH), 8.29 (s, 2H, triazole), 8.24–8.18 (m, 3H, pyr-CH), 6.30 (d, J = 9.2 Hz, 2H, Glc H-1), 5.66 (t, J = 9.4 Hz, 2H, Glc H-2), 5.51 (t, J = 9.5, 9.5 Hz, 2H, Glc H-3), 5.15 (t, J = 9.8 Hz, 2H, Glc H-4), 4.62 (m, 4H, Glc H-6,6′), 4.32 (m, 2H, Glc H-5), 4.07 (m, 4H, CH_2), 2.01 (s, 6H, OCH_3), 1.97 (s, 6H, OCH_3), 1.94 (s, 6H, OCH_3), 1.77 (s, 6H, OCH_3); ^{13}C NMR (126 MHz. DMSO-d_6): δ = 170.5, 170.0, 169.8, 168.9 (4 × OAc C═O), 163.7 (amide C═O), 148.9 (qt), 146.1 (qt), 140.0 (Pyr CH), 125.0 (Pyr CH), 122.5 (Tz CH), 84.3 (Glc C-1), 73.7 (Glc C-5), 72.7 (Glc C-3), 70.5 (Glc C-2), 68.0 (Glc C-4), 62.3 (Glc C-6), 34.9 (CH_2), 20.9, 20.8, 20.7, 20.4 (4 × OAc CH_3). IR (ATR, cm^{-1}): 1741, 1673, 1535, 1432, 1367, 1211, 1136, 1039, 953, 899, 842, 753.

$\mathbf{1Lac}^{\mathbf{OAc}}$. Synthesised following the general procedure from scaffold **2** (0.080 g, 0.33 mmol) and β-acetylazidolactose (0.436 g, 0.66 mmol). Solvent removed *in vacuo* and crude mixture precipitated from THF by dropwise addition of cold H_2O and filtered to obtain a white solid. Purified by column chromatography in 100% EtOAc (R_f = 0.16, 3rd spot) to yield a white solid. Yield: 0.589 g, 0.38 mmol (57%). HRMS (QTOF ESI+): calcd for $[M + H]^+$ $C_{65}H_{81}N_9O_{36}^+$ m/z = 1564.4857, found m/z = 1564.4868 and $[M + Na]^+$ $C_{65}H_{81}N_9O_{36}Na^+$ m/z = 1586.4676, found m/z = 1586.4678; ^{1}H NMR (500 MHz, DMSO-d_6): δ = 9.90 (t, J = 6.3 Hz, 2H, NH), 8.24–8.14 (m, 5H, Pyr and Tz), 6.21 (d, J = 9.2 Hz, 2H, Glc H-1), 5.51 (t, J = 9.4 Hz, 2H, CH), 5.24–5.20 (m, 2H, CH), 5.17 (dd, J = 10.1, 3.7 Hz, 2H, CH), 4.84 (dd, J = 10.1, 8.0 Hz, 2H, CH), 4.79 (d, J = 8.0 Hz, 2H, Gal H-1), 4.59 (t, J = 6.4 Hz, 4H, CH_2), 4.33 (d, J = 11.8 Hz, 2H, CH), 4.22 (t, J = 6.7 Hz, 2H, CH), 4.16 (t, J = 8.7 Hz, 2H, CH), 4.02–3.91 (m, 8H, Lac CH_2), 2.08 (s, 6H, OCH_3), 1.99 (s, 6H, OCH_3), 1.99 (s, 6H, OCH_3), 1.97 (s, 6H, OCH_3), 1.96 (s, 6H, OCH_3), 1.88 (s, 6H, OCH_3), 1.73 (s, 6H, OCH_3); ^{13}C NMR (126 MHz. DMSO-d_6): δ = 170.7, 170.34, 170.34, 167.0, 169.8, 169.5, 169.0 (4 × OAc C═O), 163.7 (amide C═O), 148.9 (Tz-C-1), 146.0(Pyr C-2,6), 140.0 (Pyr C-4), 124.9 (Pyr C-3,5), 122.6 (Tz C-2), 100.5 (Gal C-1), 84.1 (Glc C-1), 76.2, 74.8, 72.9, 70.8, 70.2, 69.3, 67.5 (all Lac CH), 62.7 (Lac C-6), 61.3 (Lac C-6′), 34.9 (CH_2), 21.0, 20.9, 20.8, 20.8, 20.7, 20.4 (4 × OAc CH_3); FT-IR (ATR, cm^{-1}): 1741, 1673, 1535, 1432, 1367, 1211, 1136, 1039, 953, 899, 842, 753.

General procedure for Zemplén deacetylation. Ligand $\mathbf{1}^{\mathbf{OAc}}$ was dissolved, or suspended, in methanol and to this was added 1 M NaOMe solution in MeOH (1 mL). The reaction was stirred at room temperature until TLC indicates full deprotection (*ca.* 1–2 h). Mixture was neutralised with Dowex H^+ resin, filtered and solvent removed *in vacuo*. Co-evaporation of the solvent with ethanol yielded ligands **1** as white solids.

1Gal. Deprotected $\mathbf{1Gal}^{\mathbf{OAc}}$ (1.03 g, 1.00 mmol) according to the general procedure above, giving **1Gal** as a white solid (0.645 g, 0.99 mmol, quantitative). HRMS (QTOF ESI+) calcd for $[M + H]^+$ $C_{25}H_{33}N_9O_{12}^+$ m/z = 652.2326, found m/z = 652.2320. ^{1}H NMR (500 MHz, D_2O): δ = 8.23 (s, 2H, Tz), 8.16–8.11 (d, 2H, Pyr H-2,6), 8.10–8.03 (m, 1H, Pyr H-1), 5.69 (d, J = 9.2 Hz, 2H, Gal H-1), 4.75–4.65 (m, 4H, CH2), 4.22 (t, J = 9.5 Hz, 2H, Gal H-2), 4.10 (d, J = 3.1 Hz, 2H, Gal H-4), 4.02 (t, J = 6.0 Hz, 2H, Gal H-5), 3.89 (dd, J = 9.8, 3.3 Hz, 2H, Gal H-3), 3.80 (app d, J = 6.1 Hz, 4H, Gal H6,6′) ppm. ^{13}C NMR (126 MHz, D_2O): δ = 165.6 (amide C), 147.6 (triazole C-1), 144.8 (Pyr C-5,3), 139.8 (Pyr C-1), 125.0 (Pyr C-2,6), 122.9 (triazole C-2), 88.0 (Gal C-1), 78.2 (Gal C-5), 72.9 (Gal C-3), 69.7 (Gal C-2), 68.5 (Gal C-4), 60.8 (Gal C-6), 34.4 (CH_2) ppm. IR (ATR, cm^{-1}): 3301, 2926, 1658, 1536, 1447, 1237, 1091, 1049, 884, 819, 747, 700, 643, 606.

1Glc. Deprotected $\mathbf{1Glc}^{\mathbf{OAc}}$ (0.301 g, 0.30 mmol) according to the general procedure above, giving **1Glc** as a white solid (0.195 g, 0.30 mmol, 98%). HRMS (QTOF ESI+): (QTOF ESI+) calcd for $[M + H]^+$ $C_{25}H_{33}N_9O_{12}^+$ m/z = 652.2326, found $[M + Na]^+$ m/z = 652.2331; ^{1}H NMR (400 MHz, D_2O): δ = 8.15 (s, 2H, Tz) 7.99–7.86 (m, 3H, Tz Pyr), 5.72 (d, J = 9.2 Hz, 2H, Glc H-1), 4.58 (s, 4H, CH_2), 3.99 (t, J = 9.2 Hz, 2H, Glc H-2), 3.91 (dd, J = 12.3, 1.9 Hz, 2H, Glc CH_2-6), 3.82–3.68 (m, 6H, Glc CH_2-6′, H-3, H-5), 3.65–3.58 (m, 2H, Glc H-4); ^{13}C NMR (101 MHz, D_2O): δ = 165.1 (amide C═O), 147.3 (qt), 144.6 (qt), 139.7 (Pyr CH), 124.8 (Pyr CH), 123.2 (Tz CH), 87.4 (Glc C-1), 78.8 (Glc CH), 75.8 (Glc CH), 72.2 (Glc C-2), 68.9 (Glc C-4), 60.4 (Glc CH_2-6), 34.2 (CH_2); FT-IR (ATR, cm^{-1}): 3303, 2922, 2459, 1655, 1425, 1341, 1237, 1093, 1042, 898, 842, 751, 696.

1Lac. Deprotected $\mathbf{1Lac}^{\mathbf{OAc}}$ (0.455 g, 0.29 mmol) according to the general procedure above, giving **1Lac** as a white solid

(0.230 g, 0.24 mmol, 81%). HRMS (QTOF ESI+): calcd for $C_{37}H_{53}N_9O_{22}Na^+$ $[M + Na]^+$ m/z = 998.3209, found m/z = 998.3206; ^{1}H NMR (400 MHz, D_2O): δ = 8.16 (s, 2H, Tz), 8.07–7.96 (m, 3H, Pyr), 5.61 (d, J = 9.0 Hz, 2H, Glc H-1), 4.51 (d, J = 2.5 Hz, 4H, CH_{2z}), 4.37 (d, J = 7.7 Hz, 2H, Gal H-1), 4.04 (t, J = 9.0 Hz, 2H, Lac CH), 4.00–3.90 (m, 4H, Lac CH and CH_2), 3.91–3.72 (m, 12H, Lac CH and CH_2), 3.70 (dd, J = 3.5, 9.9 Hz, 2H, Lac CH), 3.59 (dd, J = 7.7, 9.9 Hz, Hz, 2H); ^{13}C NMR (101 MHz, D_2O): δ = 165.3 (amide C═O), 147.4 (Tz C), 144.7 (Pyr C), 139.8 (Pyr CH), 124.9 (Pyr CH), 123.2 (Tz CH), 102.9 (Gal C-1), 87.2 (Glc C-1), 77.6, 77.3, 75.3, 74.5, 72.5, 71.9, 70.9, 68.5 (all Lac CH), 61.0 (Lac CH_2), 59.7 (Lac CH_2), 34.2 (CH_2); FT-IR (ATR, cm^{-1}): 3317, 2886, 1661, 1538, 1447, 1404, 1239, 1040, 1000, 895, 843, 783, 750, 697, 670.

General method for synthesis of metal complexes of ligands 1. Ligand and metal salts were dissolved in MeOH–H_2O (7 : 3) and heated, in the ratios indicated below. Eu(III) complexes were heated in microwave reactor at 90 °C for 30 minutes, while Ni(II) and Zn(II) complexes were formed by reflux overnight. Solvent was removed *in vacuo* and solids dried in oven at 60 °C.

[Eu·(1Gal)(H$_2$O)$_6$](CF$_3$SO$_3$)$_3$. Ligand **1Gal** (0.0652 g, 0.10 mmol) and $Eu(CF_3SO_3)_3$ (0.0600 g, 0.10 mmol) were reacted in a 1 : 1 molar ratio, according to the general method described above, yielding a white solid (luminescing red under UV irradiation). Yield 0.1160 g (93%). HRMS (MALDI+) calcd for $[Eu(\mathbf{1Gal}\cdot)(CF_3SO_3)_2 + Na]^+$ $C_{27}H_{33}N_9O_{18}EuCF_6S_2Na^+$ m/z = 1125.0396, found m/z = 1125.0325. ^{1}H NMR (500 MHz, D_2O): δ = 8.24 (br s, Tz), 8.15 (br app. s, Pyr), 7.91 (br app s, Pyr), 5.62–5.56 (br d, Gal H-1), 5.35, 4.25 (br s, CH2), 4.13–4.09 (br m, Gal CH), 3.97–3.95 (br m, Gal CH), 3.89–3.88 (br m, Gal CH), 3.78–3.74, 3.67–3.66 (br d, Gal Gal CH_2–6,6′); IR (ATR, cm^{-1}): 3317, 1635, 1566, 1462, 1436, 1399, 1223, 1171, 1089, 1025, 892, 811, 762, 697.

[Eu·(1Gal)$_3$](CF$_3$SO$_3$)$_3$. Ligand **1Gal** (0.0652 g, 0.10 mmol) and $Eu(CF_3SO_3)_3$ (0.0198 g, 0.03 mmol) were reacted in a 3 : 1 molar ratio, according to the general method described above, yielding a hygroscopic white solid (luminescing red under UV irradiation). Yield 0.0827 g (97%). ^{1}H NMR (500 MHz, D_2O): δ = 8.25 (br s, Tz), 8.11–7.96 (br m, Pyr), 5.62–5.54 (split d, Gal H-1), 4.60 (br s, CH_2), 4.26 (br s), 4.14–4.09 (br m, Gal CH), 3.98–3.95 (br m, Gal CH), 3.91–3.86 (br m, Gal CH), 3.78–3.74 (br m, Gal CH), 3.67–3.65 (br m, Gal CH_2–6,6′); ^{13}C NMR (126 MHz, D_2O): δ = 144.97, 122.90, 87.99, 78.24, 72.86, 69.69, 68.51, 60.82, 34.43, 16.71. IR (ATR, cm^{-1}): 3317, 2906, 1635, 1596, 1565, 1459, 1432, 1355, 1241, 1225, 1167, 1125, 1088, 1051, 1026, 890, 822, 757, 723, 699.

[Ni·(1Gal)$_2$]Cl$_2$. Ligand **1Gal** (0.0652 g, 0.10 mmol) and $NiCl_2$ (0.0065 g, 0.05 mmol) were reacted in a 2 : 1 molar ratio, according to the general method described above, yielding a lime green solid, fine powder. Yield 0.0682 g (95%). HRMS (QTOF ESI+) calcd for $[M - 2Cl]^{2+}$ $NiC_{50}H_{64}N_{18}O_{24}^+$ m/z = 679.1842, found m/z = 679.1915; ^{1}H NMR (500 MHz, D_2O): δ = 8.07 (br s, 4H, Tz), 7.97–7.90 (br m, 6H, Pyr), 5.54–5.52 (br d, 4H, Gal H-1), 4.54 (br s, 8H, CH_2), 4.08–4.04 (br t, 4H, Gal CH), 3.95–3.94 (br d, 4H, Gal CH), 3.87–3.84 (br t, 4H, Gal CH), 3.75–3.72 (br dd, 4H, Gal CH), 3.65–3.64 (br app. d, 8H, Gal CH_2–6,6′), residual EtOH. ^{13}C NMR (126 MHz, D_2O): δ = 165.6, 147.6, 144.8, 139.8, 125.0, 122.9, 88.0, 78.2, 72.9, 69.7, 68.5, 60.8, 57.4, 34.3, 16.7. IR (ATR, cm^{-1}): 3262, 2892, 1635, 1542, 1447, 1346, 1237, 1049, 881, 820, 746, 698.

[Zn·(1Gal)$_2$](OAc)$_2$. Ligand **1Gal** (0.0521 g, 0.08 mmol) and $Zn(OAc)_2$ (0.007 g, 0.04 mmol) were reacted in a 2 : 1 molar ratio, according to the general method described above, yielding a fine white hygroscopic solid (weakly fluorescent under UV irradiation). Yield 0.0569 g (92%). ^{1}H NMR (500 MHz, D_2O): δ = 8.07 (s, 4H, Tz), 7.99 (d, J = 7.0 Hz, 4H, Pyr), 7.94 (dd, J = 8.9, 6.5 Hz, 2H, Pyr), 5.53 (d, J = 9.2 Hz, 4H, Gal H-1), 4.55 (d, J = 2.0 Hz, 8H, CH_2), 4.07 (t, J = 9.5 Hz, 4H, Gal H-2), 3.95 (dd, J = 3.4, 1.1 Hz, 4H, Gal H-4), 3.86 (td, J = 6.1, 1.1 Hz, 4H, Gal H-5), 3.74 (dd, J = 9.8, 3.3 Hz, 4H, Gal H-3), 3.65 (d, J = 6.0 Hz, 8H, Gal CH_2–6,6′), 1.78 (d, J = 1.0 Hz, 3H). ^{13}C NMR (126 MHz, D_2O): δ = 165.6, 147.6, 144.8, 139.8, 125.0, 122.9, 88.0, 78.2, 72.9, 69.7, 68.5, 60.8, 34.4, 23.1. IR (ATR, cm^{-1}): 3304, 2925, 1657, 1653, 1539, 1447, 1398, 1339, 1237, 1090, 1051, 1017, 889, 843, 819, 747.

[Eu·(1Glc)(H$_2$O)$_6$](CF$_3$SO$_3$)$_3$. Ligand **1Glc** (0.020 g, 0.03 mmol) and $Eu(CF_3SO_3)_3$ (0.009 g, 0.03 mmol) were reacted in a 1 : 1 molar ratio, according to the general method described above, yielding a hygroscopic white solid (luminescing red under UV irradiation). Yield 0.0287 g (98%). ^{1}H NMR (500 MHz, D_2O): δ = 8.35 (br s, Tz), 8.23 (br s, Pyr), 5.79 (m, Gal H-1), 4.36 (br s, CH_2), 4.04–3.60 (br m, Gal CH and CH_2). IR (ATR, cm^{-1}): 3316, 2919, 2852, 1635, 1567, 1433, 1383, 1243, 1226, 1168, 1094, 1046, 1025, 897, 802, 761, 726, 696.

[Eu·(1Glc)$_3$](CF$_3$SO$_3$)$_3$. Ligand **1Glc** (0.020 g, 0.03 mmol) and $Eu(CF_3SO_3)_3$ (0.060 g, 0.10 mmol) were reacted in a 3 : 1 molar ratio, according to the general method described above, yielding a hygroscopic white solid (luminescing red under UV irradiation). Yield 0.0260 g (quantitative). ^{1}H NMR (500 MHz, D_2O): δ = 8.20 (br, s, Tz), 8.10–8.07 (br, d, pyr), 5.67–5.60 (m, Gal H-1), 4.20 (br, s, CH_2), 3.89–3.48 (br, m's, Gal CH and CH_2).

[Eu·(1Lac)(H$_2$O)$_6$](CF$_3$SO$_3$)$_3$. Ligand **1Lac** (0.0350 g, 0.035 mmol) and $Eu(CF_3SO_3)_3$ (0.0214 g, 0.035 mmol) were reacted in a 1 : 1 molar ratio, according to the general method described above, yielding a white solid (luminescing red under UV irradiation). Yield 0.0439 g (78%). ^{1}H NMR (400 MHz, D_2O): δ = 8.36–7.69 (br m, 5H, Tz Pyr), 5.85–5.56 (br split m, 2H, Glc H-1), 4.40 (d, J = 7.5 Hz, 2H, Gal H-1), 4.27 (s, 1H), 4.09–3.37 (m, 29H, Lac CH and CH_2), 2.45 (s).

[Eu·(1Lac)$_3$](CF$_3$SO$_3$)$_3$. Ligand **1Lac** (0.0350 g, 0.035 mmol) and $Eu(CF_3SO_3)_3$ (0.0072 g, 0.012 mmol) were reacted in a 3 : 1 molar ratio, according to the general method described above, yielding a white solid (luminescing orange under UV irradiation). Yield 0.0290 g (69%). ^{1}H NMR (400 MHz, D_2O): δ = 8.16–7.78 (br m, 15H, Tz and Pyr), 5.63 (br d, J = 9.1 Hz, 6H, Glc H-1), 4.56 (s, 12H, CH_2), 4.37 (d, J = 7.7 Hz, 6H, Gal H-1), 4.07–3.32 (m, 75H, Lac CH and CH_2), 0.57 (s).

Isothermal calorimetry measurements with LecA

ITC measurements were carried out on a MicroCal ITC200 (Malvern Panalytical) and the data was analyzed using the MicroCal PEAQ-ITC analysis software. The experiments were carried out at 25 °C. Ligands, *i.e.* **1Gal** and **5**, and LecA were

dissolved in the same buffer, *i.e.*, 10 mM Tris/HCl buffer (pH 7.2, 100 mM NaCl, 10 μM $CaCl_2$). The lectin concentration in the microcalorimeter cell (0.2 mL) was 300 μM. A total of 20 injections of 2 μL of 3 mM ligand solutions were added at intervals of 120 s while stirring at 750 rpm. Titrations were carried out in duplicate and K_d reported as an average.

Surface plasmon resonance measurements with LecA

Surface plasmon resonance experiments were performed on a BIACORE X100 instrument (GE Healthcare) at 25 °C. For LecA immobilization, the system was pre-equilibrated with PBS buffer (10 mM phosphate buffer pH 7.4, 2.7 mM KCl, 137 mM NaCl, 100 μM $CaCl_2$, 0.05% Tween 20), followed by an activation of the CM5 chip surface by 3 injections of 1 : 1 *N*-hydroxysuccinimide (NHS)/1-ethyl-3(3-dimethylaminopropyl)carbodiimide hydrochloride (EDC) mixture on channel 1 and 2 (contact time of 540 s, flow rate 10 μL min^{-1}) until the binding response was above 800 RU. LecA was dissolved in 10 mM sodium acetate pH 4.5 (100 μg mL^{-1}) and injected over the activated chip surface on channel 2 (contact time of 540 s, flow rate 10 μL min^{-1}) until the response of 1625 RU was reached. Excess free NHS-ester groups were capped with an injection of 1 M ethanolamine (contact time 540 s, flow rate 10 μL min^{-1}). 2.5 μM ligand stocks (*i.e.* **1Gal** and **5**) were diluted to required concentrations in a running buffer (10 mM phosphate buffer pH 7.4, 2.7 mM KCl, 137 mM NaCl, 100 μM $CaCl_2$, 0.05% Tween 20) then subjected to single-cycle kinetics analyses (contact time of 120 s and dissociation time of 120 s, flow rate 30 μL min^{-1}) consisting of injections of the analytes at 0, 3.7, 11.1, 33.3, and 100 μM over the immobilized-LecA. The chip surface was regenerated by 5× injections of 5 mM galactose followed by 5× injections of the running buffer (contact time of 120 s, flow rate 30 μL min^{-1}). K_d determination was performed using BIACORE X100 evaluation software (version 2.0) by applying the 1 : 1 binding model to fit the experimental data.

Antimicrobial assays with *P. aeruginosa*

Ligand **1Gal** and complexes were tested for their ability to inhibit growth of *P. aeruginosa* (PAO1) at various concentrations. In brief: PAO1 was seeded into wells at 10^6 CFU mL^{-1} in Mueller Hinton broth. Serial dilutions of each of the compounds was then added to the wells and a set of control wells with no compound was also set up. Each biological replicate experiment was performed in three technical replicates. Plates were incubated for 24 h at 37 °C before absorption readings at 590 nm were taken to determine the extent of inhibition of *in vitro* growth of the microorganism *versus* control.

Anti-biofilm assays with *P. aeruginosa*

Biofilm formation assays were based on methodology from previously published work.[57] In brief, starting from an overnight liquid culture in Tryptone Soya Broth, a dilution containing approximately 10^8 CFU mL^{-1} was made of PAO1 strain (kind donation from Prof. Seamas Donnelly, School of Medicine, Trinity College Dublin). For each biofilm experiment (each biological replicate), 3 wells of a round-bottomed polypropylene 96-well micro plate (Corning Costar, Sigma) were inoculated with 100 μL of this dilution, 3 wells were inoculated with the dilution and treated with the test compounds (in concentrations from 0 to 10 mM) and 3 control wells were filled with sterile medium (bacteria alone). Following 4 hours of adhesion, the supernatant, containing non-adhered cells, was removed from each well and plates rinsed using PBS solution. Following this 100 μL of fresh media was added to the control wells and fresh media with each concentration of ligand **1** or its complexes was added to the appropriate wells, the plate was then incubated for a further 24 h. After 24 h biofilm formation, the supernatants were again removed, and the wells rinsed with PBS again. Once the wells were washed, 100 μL of a 0.5% crystal violet (CV) solution was added to all wells. After 20 min, the excess CV was removed by washing the plates under running tap water. Finally, bound CV was released by adding 150 μL of 33% acetic acid (Sigma). Absorbance was measured at 590 nm.

DFT calculations for ligand and complexes

Five different conformer orientations were designed as the starting structures for the conformational analysis of the **1Gal** compound. Once the conformers were generated, they were optimised by DFT methodology using the *Gaussian16* program.[68] Geometry optimisations and vibrational frequency calculation of the **1Gal** conformers were carried out at the B3LYP-D3/6-31+g(d) computational level.[69–73] The **Europium complex** geometry optimisations and frequency calculations were performed using B3LYP with the Stuttgart-Dresden (SDD) effective core potential (ECP) on Eu and 6-31G(d,p) for light atoms (C, H, N, O), with GD3BJ dispersion correction.[74,75] For the **Nickel** and **Zinc complexes**, geometry optimisations were conducted at the B3LYP/6-31+G(d) level with GD3BJ dispersion correction. The Eu(III) complex was modelled as a septet,[76] the Ni(II) complex as a doublet,[77] and the Zn(II) complex as a singlet.[78] All the calculations were performed in water as the solvent (SMD method) and at a temperature of 298.15 K.[79] The vibrational frequencies were used to ensure that the structures were fully optimised and represented a minimum on the potential energy surface.

Adherence assays with *C. albicans*

Adherence assays were based on methodology from previously published work and will be reiterated in brief.[11] Buccal epithelial cells (BECs): cells were harvested from healthy volunteers by gently scraping the inside of the cheek with a sterile tongue depressor. Cells were washed with PBS and resuspended at a density of 1.5×10^5 mL^{-1}.

General methodology for adherence assays. For all types of assay performed, yeast cells were mixed with BECs in a ratio of 50 : 1 in a final volume of 2 mL and incubated at 37 °C for 100 minutes. The BEC/yeast cell mixture was harvested by passing through a polycarbonate membrane containing 30 μm pores which trapped the BECs but allowed unattached yeast cells to pass through. This was washed × 2 with 10 mL PBS

and cells remaining on the membrane were collected and spread on glass microscope slides which were left to slowly air dry overnight. Cells were heat fixed and stained with 0.1% (w/v) crystal violet solution, and left to air dry for 30 minutes. For each slide, the CA cells attached to 100 BECs were counted and the average number of adhered yeast cells averaged and expressed as a percentage inhibition compared to untreated controls.

Pre-treatment exclusion adherence assay. In this assay, *C. albicans* cells were treated with the glycoconjugate compounds or metal salt (*i.e.* **1Gal** and its complexes, $Eu(CF_3SO_3)_3$, $NiCl_2$, or $Zn(OAc)_2$, with a working concentration of 0.1 mM), incubated and subsequently exposed to exfoliated BECs. In brief, starting from a liquid overnight culture, 2.1×10^8 CA cells were added to Eppendorf tubes (one per compound, plus control) and the growth medium was fully removed by centrifugation followed by fresh PBS buffer washes. The clean CA cells were suspended in 900 μL PBS buffer and to them was added 100 μL of 1 mM aqueous solution of each compound tested, giving a working concentration of 0.1 mM in each sample. The Eppendorf tubes were incubated for 60 min at room temperature with occasional shaking. Then the steps described in the general methodology above were completed.

Competition adherence assay. In this assay, *C. albicans* cells, BECs and the glycoconjugate compounds or metal salts (*i.e.* **1Gal** and its complexes, $Eu(CF_3SO_3)_3$, $NiCl_2$, or $Zn(OAc)_2$, with a working concentration of 0.1 mM) were co-incubated in a shaker at 37 °C for 90 minutes before completing the steps described in the general methodology above.

Author contributions

The work was conceptualised by KW, JPB, TVT and KKa. TVT and KKa's methodologies were utilised in this article. Funding from Taighde Éireann - Research Ireland (formerly SFI and IRC) was acquired by JPB, and additional funding from French Embassy in Ireland by KW. Primary investigation was carried out by KW (synthesis, characterisation, ITC/SPR analysis, CA assays), EG (SPR), DB (DFT), KR and MJ (PA assays), KKe (synthesis, displacement assay and additional CA assays). Formal analysis of PA assay data by KR, MJ, GC, EC and JPB. Formal analysis of computational data by DB. Formal analysis of CA data by KW, KKa, KKe and JPB. Visualisation of data by KW, GC, DB, JPB. Supervision and resources were provided by JPB, GC, EC, KKa, TVT, AI and CT. Project administration by JPB. The original draft was written by KW and JPB, with reviewing and editing by GC, KKa, TVT, AI and CT.

Conflicts of interest

There are no conflicts to declare.

Data availability

The data supporting this article have been included as part of the ESI.†

Acknowledgements

This work was primarily funded by Taighde Éireann - Research Ireland under SFI Starting Investigator Research Grant (18/SIRG/5501; JPB, KW) and ITC/SPR experiments facilitated by a French Research Residency award by the French embassy in Ireland to KW to visit Grenoble (AI). We thank Irish Research Council for financial support (IRCLA/2022/3703). Support of GlycoNanoProbes and InnoGly COST Actions (CA18132 and CA18103) is also acknowledged. AI further acknowledges Glyco@Alps (ANR-15-IDEX-0002) and Labex Arcane/CBH-EUR-GS (ANR-17-EURE-0003). We thank Prof Paul Murphy for mentorship and support at University of Galway and Dr Jimmy Muldoon for mass spectroscopy support and insight, as well as technical staff in all institutions.

References

1 C. J. Murray, K. S. Ikuta, F. Sharara, L. Swetschinski, G. R. Aguilar, A. Gray, C. Han, C. Bisignano, P. Rao, E. Wool, S. C. Johnson, A. J. Browne, M. G. Chipeta, F. Fell, S. Hackett, G. Haines-Woodhouse, B. H. K. Hamadani, E. A. P. Kumaran, B. McManigal, R. Agarwal, S. Akech, S. Albertson, J. Amuasi, J. Andrews, A. Aravkin, E. Ashley, F. Bailey, S. Baker, B. Basnyat, A. Bekker, R. Bender, A. Bethou, J. Bielicki, S. Boonkasidecha, J. Bukosia, C. Carvalheiro, C. Castañeda-Orjuela, V. Chansamouth, S. Chaurasia, S. Chiurchiù, F. Chowdhury, A. J. Cook, B. Cooper, T. R. Cressey, E. Criollo-Mora, M. Cunningham, S. Darboe, N. P. J. Day, M. D. Luca, K. Dokova, A. Dramowski, S. J. Dunachie, T. Eckmanns, D. Eibach, A. Emami, N. Feasey, N. Fisher-Pearson, K. Forrest, D. Garrett, P. Gastmeier, A. Z. Giref, R. C. Greer, V. Gupta, S. Haller, A. Haselbeck, S. I. Hay, M. Holm, S. Hopkins, K. C. Iregbu, J. Jacobs, D. Jarovsky, F. Javanmardi, M. Khorana, N. Kissoon, E. Kobeissi, T. Kostyanev, F. Krapp, R. Krumkamp, A. Kumar, H. H. Kyu, C. Lim, D. Limmathurotsakul, M. J. Loftus, M. Lunn, J. Ma, N. Mturi, T. Munera-Huertas, P. Musicha, M. M. Mussi-Pinhata, T. Nakamura, R. Nanavati, S. Nangia, P. Newton, C. Ngoun, A. Novotney, D. Nwakanma, C. W. Obiero, A. Olivas-Martinez, P. Olliaro, E. Ooko, E. Ortiz-Brizuela, A. Y. Peleg, C. Perrone, N. Plakkal, A. Ponce-de-Leon, M. Raad, T. Ramdin, A. Riddell, T. Roberts, J. V. Robotham, A. Roca, K. E. Rudd, N. Russell, J. Schnall, J. A. G. Scott, M. Shivamallappa, J. Sifuentes-Osornio, N. Steenkeste, A. J. Stewardson, T. Stoeva, N. Tasak, A. Thaiprakong, G. Thwaites, C. Turner, P. Turner, H. R. van Doorn, S. Velaphi, A. Vongpradith, H. Vu, T. Walsh, S. Waner,

T. Wangrangsimakul, T. Wozniak, P. Zheng, B. Sartorius, A. D. Lopez, A. Stergachis, C. Moore, C. Dolecek and M. Naghavi, *Lancet*, 2022, **399**, 629–655.

2 WHO, *2021 Antibacterial agents in clinical and preclinical development: an overview and analysis*, World Health Organization, Geneva, 2022.

3 E. Tacconelli, E. Carrara, A. Savoldi, S. Harbarth, M. Mendelson, D. L. Monnet, C. Pulcini, G. Kahlmeter, J. Kluytmans, Y. Carmeli, M. Ouellette, K. Outterson, J. Patel, M. Cavaleri, E. M. Cox, C. R. Houchens, M. L. Grayson, P. Hansen, N. Singh, U. Theuretzbacher, N. Magrini, A. O. Aboderin, S. S. Al-Abri, N. A. Jalil, N. Benzonana, S. Bhattacharya, A. J. Brink, F. R. Burkert, O. Cars, G. Cornaglia, O. J. Dyar, A. W. Friedrich, A. C. Gales, S. Gandra, C. G. Giske, D. A. Goff, H. Goossens, T. Gottlieb, M. G. Blanco, W. Hryniewicz, D. Kattula, T. Jinks, S. S. Kanj, L. Kerr, M. P. Kieny, Y. S. Kim, R. S. Kozlov, J. Labarca, R. Laxminarayan, K. Leder, L. Leibovici, G. Levy-Hara, J. Littman, S. Malhotra-Kumar, V. Manchanda, L. Moja, B. Ndoye, A. Pan, D. L. Paterson, M. Paul, H. Qiu, P. Ramon-Pardo, J. Rodríguez-Baño, M. Sanguinetti, S. Sengupta, M. Sharland, M. Si-Mehand, L. L. Silver, W. Song, M. Steinbakk, J. Thomsen, G. E. Thwaites, J. W. van der Meer, N. V. Kinh, S. Vega, M. V. Villegas, A. Wechsler-Fördös, H. F. L. Wertheim, E. Wesangula, N. Woodford, F. O. Yilmaz and A. Zorzet, *Lancet Infect. Dis.*, 2018, **18**, 318–327.

4 WHO, *WHO fungal priority pathogens list to guide research, development and public health action*, World Health Organization, 2022.

5 S. Sattin and A. Bernardi, *Trends Biotechnol.*, 2016, **34**, 483–495.

6 M. B. Calvert, V. R. Jumde and A. Titz, *Beilstein J. Org. Chem.*, 2018, **14**, 2607–2617.

7 S. Behren and U. Westerlind, *Molecules*, 2019, **24**, 1004.

8 K. Wojtczak and J. P. Byrne, *ChemMedChem*, 2022, **17**, e202200081.

9 U. Theuretzbacher and L. J. V. Piddock, *Cell Host Microbe*, 2019, **26**, 61–72.

10 S. Kleeb, L. Pang, K. Mayer, D. Eris, A. Sigl, R. C. Preston, P. Zihlmann, T. Sharpe, R. P. Jakob, D. Abgottspon, A. S. Hutter, M. Scharenberg, X. Jiang, G. Navarra, S. Rabbani, M. Smiesko, N. Lüdin, J. Bezençon, O. Schwardt, T. Maier and B. Ernst, *J. Med. Chem.*, 2015, **58**, 2221–2239.

11 H. Martin, M. M. Govern, L. Abbey, A. Gilroy, S. Mullins, S. Howell, K. Kavanagh and T. Velasco-Torrijos, *Eur. J. Med. Chem.*, 2018, **160**, 82–93.

12 J. L. Reymond, M. Bergmann and T. Darbrea, *Chem. Soc. Rev.*, 2013, **42**, 4814–4822.

13 M. Bergmann, G. Michaud, R. Visini, X. Jin, E. Gillon, A. Stocker, A. Imberty, T. Darbre and J. L. Reymond, *Org. Biomol. Chem.*, 2015, **14**, 138–148.

14 A. M. Boukerb, A. Rousset, N. Galanos, J.-B. Méar, M. Thépaut, T. Grandjean, E. Gillon, S. Cecioni, C. Abderrahmen, K. Faure, D. Redelberger, E. Kipnis, R. Dessein, S. Havet, B. Darblade, S. E. Matthews, S. de Bentzmann, B. Guéry, B. Cournoyer, A. Imberty and S. Vidal, *J. Med. Chem.*, 2014, **57**, 10275–10289.

15 E. Zahorska, S. Kuhaudomlarp, S. Minervini, S. Yousaf, M. Lepsik, T. Kinsinger, A. K. H. Hirsch, A. Imberty and A. Titz, *Chem. Commun.*, 2020, **56**, 8822–8825.

16 R. Sommer, D. Hauck, A. Varrot, S. Wagner, A. Audfray, A. Prestel, H. M. Möller, A. Imberty and A. Titz, *ChemistryOpen*, 2015, **4**, 756–767.

17 M. Duca, D. Haksar, J. van Neer, D. M. E. Thies-Weesie, D. Martínez-Alarcón, H. de Cock, A. Varrot and R. J. Pieters, *ACS Chem. Biol.*, 2022, **17**, 3515–3526.

18 P. A. Roberts, R. M. Huebinger, E. Keen, A.-M. Krachler and S. Jabbari, *PLoS Comput. Biol.*, 2019, **15**, e1007211.

19 G. Michaud, R. Visini, M. Bergmann, G. Salerno, R. Bosco, E. Gillon, B. Richichi, C. Nativi, A. Imberty, A. Stocker, T. Darbre and J. L. Reymond, *Chem. Sci.*, 2015, **7**, 166–182.

20 H.-P. Hauber, M. Schulz, A. Pforte, D. Mack, P. Zabel, U. Schumacher, P. D. Med and H.-P. Hauber, *Int. J. Med. Sci.*, 2008, **5**, 371–376.

21 I. Bucior, J. Abbott, Y. Song, M. A. Matthay and J. N. Engel, *Am. J. Physiol.*, 2013, **305**, L352.

22 D. Sharma, L. Misba and A. U. Khan, *Antimicrob. Resist. Infect. Control*, 2019, **8**, 76.

23 F. Pertici and R. J. Pieters, *Chem. Commun.*, 2012, **48**, 4008–4010.

24 F. Pertici, N. J. D. Mol, J. Kemmink and R. J. Pieters, *Chem. – Eur. J.*, 2013, **19**, 16923–16927.

25 A. Vitiello, F. Ferrara, M. Boccellino, A. Ponzo, C. Cimmino, E. Comberiati, A. Zovi, S. Clemente and M. Sabbatucci, *Biomedicines*, 2023, **11**, 1063.

26 S. Fairuz, R. S. Nair and N. Billa, *Pharmaceutics*, 2022, **14**, 1823.

27 R. Kovács and S. Mahmoudi, *Front. Cell. Infect. Microbiol.*, 2023, **13**, 1184922.

28 H. Martin, T. Somers, M. Dwyer, R. Robson, F. M. Pfeffer, R. Bjornsson, T. Krämer, K. Kavanagh and T. Velasco-Torrijos, *RSC Med. Chem.*, 2020, **11**, 1386–1401.

29 H. Martin, D. Goyard, A. Margalit, K. Doherty, O. Renaudet, K. Kavanagh and T. Velasco-Torrijos, *Bioconjugate Chem.*, 2021, **32**, 971–982.

30 E. J. Anthony, E. M. Bolitho, H. E. Bridgewater, O. W. L. Carter, J. M. Donnelly, C. Imberti, E. C. Lant, F. Lermyte, R. J. Needham, M. Palau, P. J. Sadler, H. Shi, F.-X. Wang, W.-Y. Zhang and Z. Zhang, *Chem. Sci.*, 2020, **11**, 12888–12917.

31 K. D. Mjos and C. Orvig, *Chem. Rev.*, 2014, **114**, 4540–4563.

32 A. Frei, J. Zuegg, A. G. Elliott, M. Baker, S. Braese, C. Brown, F. Chen, C. G. Dowson, G. Dujardin, N. Jung, A. P. King, A. M. Mansour, M. Massi, J. Moat, H. A. Mohamed, A. K. Renfrew, P. J. Rutledge, P. J. Sadler, M. H. Todd, C. E. Willans, J. J. Wilson, M. A. Cooper and M. A. T. Blaskovich, *Chem. Sci.*, 2020, **11**, 2627–2639.

33 A. Frei, A. G. Elliott, A. Kan, H. Dinh, S. Bräse, A. E. Bruce, M. R. Bruce, F. Chen, D. Humaidy, N. Jung, A. P. King, P. G. Lye, H. K. Maliszewska, A. M. Mansour, D. Matiadis, M. P. Muñoz, T.-Y. Pai, S. Pokhrel, P. J. Sadler, M. Sagnou,

M. Taylor, J. J. Wilson, D. Woods, J. Zuegg, W. Meyer, A. K. Cain, M. A. Cooper and M. A. T. Blaskovich, *JACS Au*, 2022, **2**, 2277–2294.

34 D. J. Barillo, A. R. Barillo, S. Korn, K. Lam and P. S. Attar, *Burns*, 2017, **43**, 1189–1194.

35 A. Evans and K. A. Kavanagh, *J. Med. Microbiol.*, 2021, **70**, 001363.

36 M. A. Malik, S. A. Lone, M. Y. Wani, Md. I. A. Talukdar, O. A. Dar, A. Ahmad and A. A. Hashmi, *Bioorg. Chem.*, 2020, **98**, 103771.

37 X. Li, K. Heimann, F. Li, J. M. Warner, F. R. Keene and J. G. Collins, *Dalton Trans.*, 2016, **45**, 4017–4029.

38 F. Li, J. G. Collins and F. R. Keene, *Chem. Soc. Rev.*, 2015, **44**, 2529–2542.

39 S. V. Kumar, S. O. Scottwell, E. Waugh, C. J. McAdam, L. R. Hanton, H. J. L. Brooks and J. D. Crowley, *Inorg. Chem.*, 2016, **55**, 9767–9777.

40 S. Li, C. Wu, X. Tang, S. Gao, X. Zhao, H. Yan and X. Wang, *Sci. China: Chem.*, 2013, **56**, 595–603.

41 P. Rogala, G. Czerwonka, S. Michałkiewicz, M. Hodorowicz, B. Barszcz and A. Jabłońska-Wawrzycka, *Chem. Biodivers.*, 2019, **16**, e1900403.

42 G. Czerwonka, D. Gmiter, A. Guzy, P. Rogala, A. Jabłońska-Wawrzycka, A. Borkowski, T. Cłapa, D. Narożna, P. Kowalczyk, M. Syczewski, M. Drabik, M. Dańczuk and W. Kaca, *Biofouling*, 2019, **35**, 59–74.

43 M. Orsi, B. S. Loh, C. Weng, W. H. Ang and A. Frei, *Angew. Chem., Int. Ed.*, 2024, **63**, e202317901.

44 D. Iacopini, J. Vančo, S. Di Pietro, V. Bordoni, S. Zacchini, F. Marchetti, Z. Dvořák, T. Malina, L. Biancalana, Z. Trávníček and V. Di Bussolo, *Bioorg. Chem.*, 2022, **126**, 105901.

45 S. Thangamani, H. Mohammad, M. F. N. Abushahba, T. J. P. Sobreira, V. E. Hedrick, L. N. Paul and M. N. Seleem, *Sci. Rep.*, 2016, **6**, 22571.

46 E. Sauvageot, M. Elie, S. Gaillard, R. Daniellou, P. Fechter, I. J. Schalk, V. Gasser, J.-L. Renaud and G. L. A. Mislin, *Metallomics*, 2017, **9**, 1820–1827.

47 C. O'Reilly, S. Blasco, B. Parekh, H. Collins, G. Cooke, T. Gunnlaugsson and J. P. Byrne, *RSC Adv.*, 2021, **11**, 16318–16325.

48 M. J. Celestine, J. L. Bullock, S. Boodram, V. H. Rambaran and A. A. Holder, *Rev. Inorg. Chem.*, 2015, **35**, 57–67.

49 D. E. Barry, D. F. Caffrey and T. Gunnlaugsson, *Chem. Soc. Rev.*, 2016, **45**, 3244–3274.

50 K. Wojtczak, E. Zahorska, I. J. Murphy, F. Koppel, G. Cooke, A. Titz and J. P. Byrne, *Chem. Commun.*, 2023, **59**, 8384–8387.

51 A. Imberty, M. Wimmerová, E. P. Mitchell and N. Gilboa-Garber, *Microbes Infect.*, 2004, **6**, 221–228.

52 For Tb(III) complexes of **1Gal** and **5**, K_d with LecA was determined by ITC as 13.6 and 11.1, respectively.

53 O. Kotova, J. A. Kitchen, C. Lincheneau, R. D. Peacock and T. Gunnlaugsson, *Chem. – Eur. J.*, 2013, **19**, 16181–16186.

54 A. T. O'Neil, N. Zhang, J. A. Harrison, S. M. Goldup and J. A. Kitchen, *Supramol. Chem.*, 2021, **33**, 160–173.

55 Hydration number (q), determined by measuring luminescent lifetime in D_2O (3.00 ms) and H_2O (0.180). Applying modified Horrock's equation, q=5.5 ± 0.5. Six coordinated water molecules is analogous to our previously-reported Tb (III) complexes, ref. 50. See also: T. Ala-Kleme, *et al.*, *Lanthanide Luminescence Photophysical, Analytical and Biological Aspects*, Springer Verlag, Heidelberg, 2011; A. Beeby, I. M. Clarkson, R. S. Dickins, S. Faulkner, D. Parker, L. Royle, A. S. de Sousa, J. A. G. Williams and M. Woods, *J. Chem. Soc., Perkin Trans. 2*, 1999, 493–504.

56 A. Chauvin, F. Gumy, D. Imbert and J. G. Bünzli, *Spectrosc. Lett.*, 2004, **37**, 517–532.

57 E. Peeters, H. J. Nelis and T. Coenye, *J. Microbiol. Methods*, 2008, **72**, 157–165.

58 D. A. Capdevila, J. Wang and D. P. Giedroc, *J. Biol. Chem.*, 2016, **291**, 20858–20868.

59 C. Chemani, A. Imberty, S. D. Bentzmann, M. Pierre, M. Wimmerová, B. P. Guery and K. Faure, *Infect. Immun.*, 2009, **77**, 2065–2075.

60 B. Đ. Glišić, L. Senerovic, P. Comba, H. Wadepohl, A. Veselinovic, D. R. Milivojevic, M. I. Djuran and J. Nikodinovic-Runic, *J. Inorg. Biochem.*, 2016, **155**, 115–128.

61 M. K. Hostetter, *Clin. Microbiol. Rev.*, 1994, **7**, 29–42.

62 B. Timmermans, A. De Las Peñas, I. Castaño and P. Van Dijck, *J. Fungi*, 2018, **4**, 60.

63 G. Cotter and K. Kavanagh, *Br. J. Biomed. Sci.*, 2000, **57**, 241–249.

64 Y. Fukazawa and K. Kagaya, *J. Med. Vet. Mycol.*, 1997, **35**, 87–99.

65 T. Ziegler and C. Hermann, *Tetrahedron Lett.*, 2008, **49**, 2166–2169.

66 F. M. Ibatullin and K. A. Shabalin, *Synth. Commun.*, 2000, **30**, 2819–2823.

67 S. Kuhaudomlarp, E. Gillon, A. Varrot and A. Imberty, in *Lectin Purification and Analysis: Methods and Protocols*, ed. J. Hirabayashi, Springer US, New York, NY, 2020, pp. 257–266.

68 M. J. Frisch, G. W. Trucks, H. B. Schlegel, G. E. Scuseria, M. A. Robb, J. R. Cheeseman, G. Scalmani, V. Barone, G. A. Petersson, H. Nakatsuji, X. Li, M. Caricato, A. V. Marenich, J. Bloino, B. G. Janesko, R. Gomperts, B. Mennucci, H. P. Hratchian, J. V. Ortiz, A. F. Izmaylov, J. L. Sonnenberg, D. Williams-Young, F. Ding, F. Lipparini, F. Egidi, J. Goings, B. Peng, A. Petrone, T. Henderson, D. Ranasinghe, V. G. Zakrzewski, J. Gao, N. Rega, G. Zheng, W. Liang, M. Hada, M. Ehara, K. Toyota, R. Fukuda, J. Hasegawa, M. Ishida, T. Nakajima, Y. Honda, O. Kitao, H. Nakai, T. Vreven, K. Throssell, J. A. Montgomery Jr., J. E. Peralta, F. Ogliaro, M. J. Bearpark, J. J. Heyd, E. N. Brothers, K. N. Kudin, V. N. Staroverov, T. A. Keith, R. Kobayashi, J. Normand, K. Raghavachari, A. P. Rendell, J. C. Burant, S. S. Iyengar, J. Tomasi, M. Cossi, J. M. Millam, M. Klene, C. Adamo, R. Cammi, J. W. Ochterski, R. L. Martin, K. Morokuma, O. Farkas, J. B. Foresman and D. J. Fox, *Gaussian 16 Rev. C.01*, 2016.

69 A. D. Becke, *J. Chem. Phys.*, 1993, **98**, 5648–5652.

70 S. Grimme, S. Ehrlich and L. Goerigk, *J. Comput. Chem.*, 2011, **32**, 1456–1465.
71 W. J. Hehre, R. Ditchfield and J. A. Pople, *J. Chem. Phys.*, 1972, **56**, 2257–2261.
72 P. C. Hariharan and J. A. Pople, *Theor. Chim. Acta*, 1973, **28**, 213–222.
73 S. Grimme, J. Antony, S. Ehrlich and H. Krieg, *J. Chem. Phys.*, 2010, **132**(15), 154104.
74 X. Cao and M. Dolg, *J. Chem. Phys.*, 2001, **115**, 7348–7355.
75 X. Cao and M. Dolg, *J. Mol. Struct.: THEOCHEM*, 2002, **581**, 139–147.
76 S. Carlotto, L. Babetto, M. Bortolus, A. Carlotto, M. Rancan, G. Bottaro, L. Armelao, D. Carbonera and M. Casarin, *Inorg. Chem.*, 2021, **60**, 15141–15150.
77 J. L. Mancuso, C. A. Gaggioli, L. Gagliardi and C. H. Hendon, *J. Phys. Chem. C*, 2021, **125**, 22036–22043.
78 J. G. O. Neto, J. R. Viana, J. B. O. Lopes, A. D. S. G. Lima, M. L. Sousa, M. R. Lage, S. R. Stoyanov, R. Lang and A. O. Santos, *J. Mol. Model.*, 2022, **28**, 341.
79 A. V. Marenich, C. J. Cramer and D. G. Truhlar, *J. Phys. Chem. B*, 2009, **113**, 6378–6396.